β-Amyloid Amorphous Aggregates Induced by the Small Natural Molecule Ferulic Acid

ARTICLE *in* THE JOURNAL OF PHYSICAL CHEMISTRY B · OCTOBER 2013

Impact Factor: 3.3 · DOI: 10.1021/jp4079986 · Source: PubMed

5 AUTHORS, INCLUDING:

Emilia Bramanti
Italian National Research Council
123 PUBLICATIONS **1,742** CITATIONS
SEE PROFILE

Francesco Lenci
Italian National Research Council
97 PUBLICATIONS **1,613** CITATIONS
SEE PROFILE

THE JOURNAL OF PHYSICAL CHEMISTRY B

Article

pubs.acs.org/JPCB

β-Amyloid Amorphous Aggregates Induced by the Small Natural Molecule Ferulic Acid

Emilia Bramanti,[†] Lorenzo Fulgentini,[‡,§] Ranieri Bizzarri,[‡] Francesco Lenci,[‡] and Antonella Sgarbossa*[,‡]

[†]Istituto dei Composti Organo-Metallici, [‡]Istituto di Biofisica, and [§]Istituto Nazionale di Ottica, CNR, U.O. Pisa, Via G. Moruzzi, 1, 56124, Pisa, Italy

ABSTRACT: There is an emerging interest in small natural molecules for their potential therapeutic use in neurodegenerative disorders like Alzheimer's disease (AD). Ferulic acid (FA), an antioxidant phenolic compound present in fruit and vegetables, has been proposed as an inhibitor of beta amyloid (Aβ) pathological aggregation. Using fluorescence and Fourier transform infrared spectroscopy, electrophoresis techniques, chromatographic analysis, and confocal microscopy, we investigated the effects of FA in the early stages of Aβ fibrillogenesis in vitro. Our results show that FA interacts promptly with Aβ monomers/oligomers, interfering since the beginning with its self-assembly and finally forming amorphous aggregates more prone to destabilization. These findings highlight the molecular basis underlying FA antiamyloidogenic activity in AD.

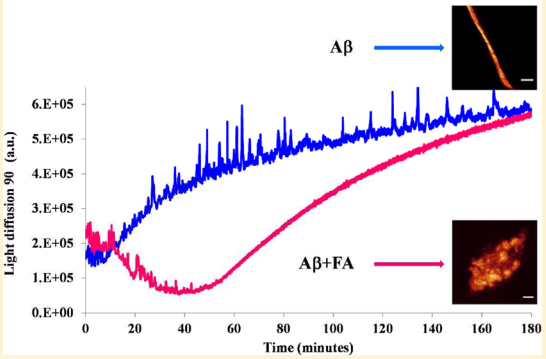

INTRODUCTION

Amyloid-β peptide (Aβ) fibrils are characteristic hallmarks of Alzheimer's disease (AD) in brain. The plaque and vascular amyloid deposits of AD are mainly composed of the 42 and 40 residue Aβ (Aβ42 and Aβ40 respectively) that are generated constitutively by sequential proteolysis of the β-amyloid precursor protein (APP) by the β- and γ-secretase enzymes. High levels of both Aβ40 and Aβ42 were found to be associated with AD.[1] Converging evidence points out that the overproduction and the abnormal self-aggregation of Aβ trigger the AD pathogenic cascade.[2,3] The aggregation pathway proceeds from Aβ monomers with a prevalent random coil secondary structure to the formation of oligomers and then of ordered protofibrils and fibrils possessing a β-sheet conformation. The soluble oligomers seem to be the main neurotoxic species,[4,5] apparently capable of forming nonspecific pore-like channels in neuron membranes, thereby inducing cell dysfunction.[6] Amyloid fibrils too are able to trigger cellular toxicity, although to a lesser extent in comparison with oligomeric species. In fact, they can directly interact with cell membrane lipids and be destabilized and disassembled into the pre-fibrillar toxic forms.[7] Amyloid fibrils appear as long fibers composed of numerous twisted filaments in which repeating substructure consists of β-strands that run perpendicular to the fiber axis, forming a cross-β sheet of variable length.[8] A widely used diagnostic test for revealing the presence of amyloid fibrils in vivo or in vitro relies on the changes in the fluorescent properties of the benzothiazole dye thioflavin T (ThT) upon binding the fibrillar structures. The general assumption is that the Aβ fibrils constrain ThT in a rigid environment, thereby hampering the nonradiative deactivation channel of ThT related to the intramolecular twist between the benzothiazole and aminobenzene rings.[9] To date there are still no effective treatments to prevent, arrest, or reverse AD.[10,11] Promising therapeutical strategies come from the combined actions of antioxidants and inhibitors of Aβ fibril formation.[12−16] In this perspective, the antioxidant ferulic acid (FA) (Figure 1), a small phenolic molecule present in fruit and vegetables, on account of its slow toxicity and strong antioxidant properties,[17] stands out as an extremely interesting small biomolecule with neuroprotective activity.[18] A novel aspect of the neuroprotective effect of FA was investigated in the organ of Corti of guinea pigs exposed to noise damage. It has been shown that FA is able not only to scavenge free radicals but also to enhance the cell stress response by the up-regulation of the antioxidant enzyme heme oxygenase-1.[19] Moreover, the long-term administration of FA was shown to provide effective protection against neurotoxicity induced in mice by centrally administered Aβ in vivo.[20] Solid lipid nanoparticles containing FA, developed as a novel drug delivery system to the brain, were found to decrease oxidative stress and cell death induced by Aβ.[21] Ono and coworkers suggested that the inhibition of formation and destabilization of amyloid fibrils is caused by the direct binding of FA to these structures, although the molecular mechanisms underlying its

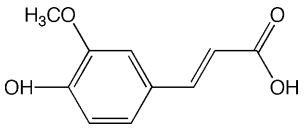

Figure 1. Chemical formula of ferulic acid (FA).

Received: August 9, 2013
Revised: October 9, 2013

   dx.doi.org/10.1021/jp4079986 | J. Phys. Chem. B XXXX, XXX, XXX−XXX

antiamyloidogenic activity remained to be clarified.[22−25] In a previous paper of ours, we investigated the effect of FA on preformed fibrils: a clear disaggregation effect of FA on preformed amyloid fibrils was shown by means of experimental and computational techniques. In particular, we demonstrated that FA has disruptive effects on the Aβ preformed fibrils redirecting the organized fibrillar conformation toward amorphous aggregates by means of hydrogen bonding and hydrophobic interactions with the various regions of the oligopeptide assembly. FA molecules cover the fibrillar structure and show a slight tendency to insert their carboxyl and hydroxyl moieties between the Aβ peptide chains. This effect could limit or even hinder the association of incoming Aβ peptides and thus inhibit fibrillogenesis as well as their reassociation in the association−dissociation dynamic equilibrium.[26] In the present work, we evaluated the influence of FA on the amyloid oligomerization/aggregation pathway since the very early stages of its self-assembly to establish if FA can prevent and thus act as an inhibitor of the fibrillogenesis phenomenon. With the aim of getting new physical insights into the molecular basis underlying FA antiamyloidogenic activity, we investigated the in vitro effects of FA on Aβ (1−40) oligomerization and fibril formation process and on peptide conformational evolution by means of several experimental techniques such as fluorescence spectroscopy, Fourier transform infrared spectroscopy (FTIR), photoinduced cross-linking of unmodified proteins (PICUP), followed by SDS-PAGE, size exclusion chromatography (SEC), and confocal microscopy.

EXPERIMENTAL METHODS

Sample Preparation. Aβ40 peptides were purchased from Biopeptide (San Diego, CA), Thioflavin T (ThT, T3516) and *trans*-ferulic acid (128708, 99% purity) were purchased from Sigma-Aldrich (Milan, Italy). Aβ40 was dissolved in NaOH 2 mM (pH 10.5), sonicated for 10 min, and lyophilized according to Fezoui et al.[27] For measurements, the powder was instantly dissolved in 0.15 M NaCl Milli-Q water solution (pH 6.5). Ferulic acid stock solution (3.3 mM) was dissolved in water.

Aggregation Kinetics. 75 μM Aβ40 was dissolved in 0.15 M NaCl Milli-Q water solution, and its aggregation was induced by increasing the temperature to 45 °C under continuous stirring in the thermostatic cell holder of a FLUOROMAX 4 HORIBA-Jobin Yvon spectrofluorimeter. FA-treated Aβ was spiked with 330 μM FA and incubated at 45 °C. The aggregation process was monitored by setting both the excitation and the emission monochromator at 405 nm and measuring light diffusion at 90°(LD) for 6 h.[28,29] In our system the illuminated volume was a cylinder of 20 μL. (The total volume of the solution in the microcuvette is 800 μL continuously stirred.) For such a large volume, fluctuations of diffused light reflect a very few large particles floating in the solution. Assuming a Poissonian distribution, we may estimate that in 20 μL fluctuations should arise from particle concentration as low as $\sim 10^{-17}$ M. Therefore, we can safely assume that monomers and small oligomers are the largely predominant species in our systems.

ThT Fluorescence Assay. ThT assay was performed measuring fluorescence emission spectra (λ_{exc} = 442 nm) of 5 μM ThT aqueous solutions in the presence of Aβ and FA-treated Aβ at t = 0 and 6 h of the aggregation kinetics. We added 50 μL of 75 μM Aβ40 with and without 330 μM FA to 850 μL of ThT solution at 5 μM final concentration. Thus, we reached 4 μM Aβ40 and 5 μM ThT final concentrations.

Photoinduced Cross-Linking of Unmodified Proteins and SDS-PAGE. Peptides were centrifuged at 11 000*g* for 10 min, and the surnatant was covalently cross-linked using PICUP according to Fancy and Kodadek.[30] The cross-linked oligomer mixtures were fractionated by SDS-PAGE using 10−20% Tricine gels (1.0 mm thick, 10 wells) and silver-stained.

Fourier Transform Infrared Spectroscopy. Infrared spectra were recorded by using a Perkin-Elmer Spectrum One FTIR spectrophotometer equipped with a TGS detector. For each sample, 128 interferograms were recorded, averaged and Fourier-transformed to produce a spectrum with a nominal resolution of 4 cm^{-1}. Spectrum software (Perkin-Elmer) and a written-in house LabVIEW program for peak fitting were employed to run and process spectra, respectively.[30] Secondary structures were estimated by expressing the amplitude value of the bands assigned to each of these structures as a fraction of the total sum of the amplitudes of the amide I components.[26,29,32] FTIR spectra were recorded on three independent samples for each condition investigated (Aβ40 with and without 330 μM FA at t = 0 and 6 h)

Size Exclusion Chromatography. For SEC analysis, carbonic anhydrase from bovine erythrocytes (CA, 21803), bovine serum albumin (BSA, A-0281), albumin from chicken egg white (OVA, A-5503), human serum albumin (HSA, A-1887), β-lactoglobulin (β-LG, L-3908) and α-lactalbumin from bovine milk (α-Lac, L-6010), myoglobin from equine skeletal muscle (Myo, M-0630), α-chymotrypsinogen A from bovine pancreas (α-Chy, C-4879), lysozyme from chicken egg white (Lys, L-6876), human hemoglobin (Hb, H-7379), aprotinin from bovine lung (10820), and cytochrome *c* from equine heart (Cyt C, C-7752) were purchased from Sigma Aldrich Fluka (Milan, Italy). The buffer solutions contained 50 mM phosphate pH 7.4 (PBS). The stock solutions of proteins for SEC column calibration were prepared by dissolving the protein (1−5 mg of the lyophilized powder) in 50 mM PBS pH 7.4, 0.15 M NaCl. Water deionized with a Milli-Q system was used throughout and degassed prior to use. SEC analysis of soluble fraction of Aβ peptide solutions was performed using a P4000 pump (ThermoFinnigan) equipped with a Rheodyne 7125 injector (Rheodyne, Cotati, CA), a 50 μL poly(etheretherketone) (PEEK tubing, Upchurch, Oak Harbor, WA) injection loop, a UV6000 diode array detector (ThermoFinnigan), and a FL3000 (ThermoFinnigan) fluorescence detector. Standard proteins of known molecular weight (MW) were injected in an SEC Biosep SEC S2000 column (Phenomenex, 300 × 7.8 mm, 1000−300 000 Da MW range) for column calibration. Separation was performed using an isocratic elution in 100% 50 mM PBS pH 7.0, 0.15 M NaCl at 1.0 mL/min. Aβ samples were centrifuged at 11 000*g* for 10 min, and the surnatant was injected in the chromatographic system.

Confocal Microscopy. Imaging of Aβ fibril bundles and FA-Aβ complexes stained with ThT was carried out using a Leica TCS SL inverted laser scanning confocal microscope (Leica Microsystems AG, Wetzlar, Germany) interfaced with an Ar laser for excitation at 458 nm and adopting a 63 × 1.4NA numerical aperture oil immersion objective (Leica Microsystems). Aβ fibril bundles and FA-Aβ complexes were left to settle down for 20 min from solution in 3.5 cm glass-bottomed Petri dishes (WillCo-Dish; WillCo Wells, Amsterdam, The Netherlands) and then imaged therein. Acquisition parameters were: excitation power 50−200 μW at objective, 400 Hz line scanning speed, and 470−515 nm collection wavelength range.

dx.doi.org/10.1021/jp4079986 | J. Phys. Chem. B XXXX, XXX, XXX−XXX

Transmission images were obtained in differential image contrast mode (Nomarski image) by using the same laser source. All images were 512 × 512 pixels in size, and fluorescence intensity was represented by a "glow" pseudocolor scale.

RESULTS AND DISCUSSION

The time course of 75 μM Aβ40 self-assembly was followed both with and without 330 μM FA. It should be noted that Aβ40 is natively unfolded and very prone to aggregation, and whereas at nanomolar concentrations oligomerization and fibril formation do not occur, at micromolar concentrations it is difficult to obtain pure monomers. As stated in the Experimental Methods section, for Aβ preparation we followed the Fezoui procedure,[27] which has been demonstrated to produce peptide solutions containing higher yields of monomer and low-order oligomer states (low molecular weight, LMW, Aβ) and lower concentration levels of pre-existent aggregates or seeds present in the peptide stocks. So, under our experimental conditions, at t = 0 and T = 25 °C a mixture of monomers and oligomers (dimers, trimers, and tetramers) of Aβ is probably in equilibrium. Under our experimental conditions, increasing the temperature from 25 to 45 °C, the aggregation of Aβ40 started out after a few minutes and leveled off in 6 h, as highlighted by LD (Figure 2). In the presence of 330 μM FA, the Aβ40 time-

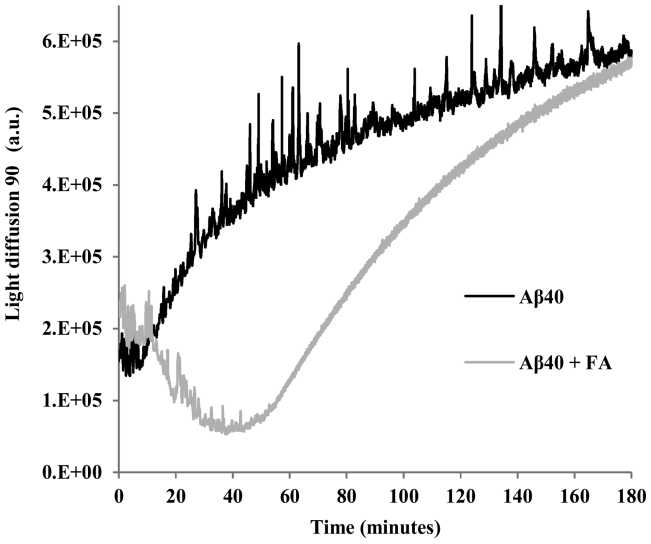

Figure 2. Time course (the first 3 h) of the light diffusion at 90° at T = 45 °C of 75 μM Aβ40 in 0.15 M NaCl without (black) and with (gray) 330 μM FA.

course was rather different, showing two phases: from 0 to 40 min, we observed a decrease in LD, suggesting assembly reversal or formation of small-sized species; from 40 min to 6 h, the signal increased, indicating the formation of larger or more numerous aggregates. It is worth noting that reducing the FA concentration to 150, 75, or 33 μM did not significantly alter the Aβ40 kinetic aggregation pattern (data not shown). The initial drop in both kinetic traces of Aβ40 with and without FA, observed in the first minutes of the experiments, has to be attributed to the perturbation of the initial equilibrium due to the increase in temperature (from 25 to 45 °C). It should also be noted that the further decay observed for FA-treated sample is not due to fibril deposition in the cuvette because the solutions are kept stirred. Because monomers and oligomers coexist at t = 0, under our experimental conditions, it can be hypothesized that in the first 40 min FA contributes to oligomers disassembly. However, for longer times FA induces the formation of aggregates that contribute to LD signal. The fact that after 40 min the kinetic trace of FA-treated sample is smoother than that of the untreated sample may indicate the absence of very large aggregates.

Thioflavin T (ThT) assay was performed on Aβ40- and FA-treated Aβ40 at t = 0 and 6 h (Figure 3). At t = 0, no ThT

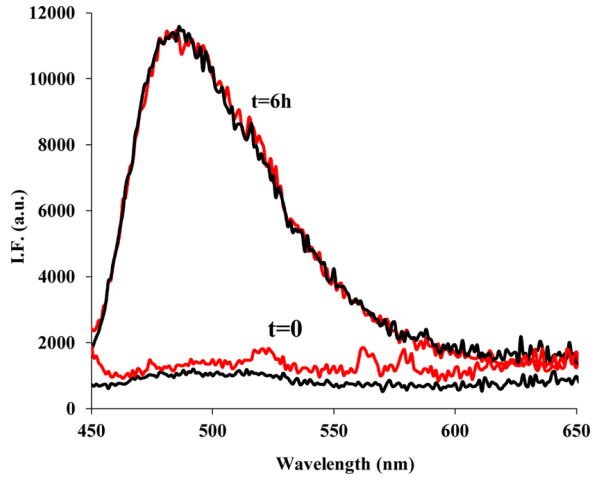

Figure 3. Fluorescence emission spectra (λ_{exc} = 442 nm) of 5 μM ThT in the presence of Aβ40 (black) and FA-treated Aβ40 (red) at t = 0 and 6 h. Intensity of fluorescence (I.F.) in arbitrary units (a.u.).

fluorescence was detected in both samples. Remarkably, at t = 6 h, the ThT fluorescence intensities reached the same value with and without FA. Because ThT is considered a specific marker of amyloid fibril formation, this finding at first sight may suggest that a similar degree of fibrillogenesis is ultimately reached both with and without FA. ThT control assay performed on FA alone before and after 6 h of incubation at 45 °C excluded the occurrence of artifacts or fluorescent complexes between FA and ThT (data not shown).

To get morphological information on the shape of the aggregates positive to ThT assay, a confocal microscopy investigation was performed on FA-treated and untreated Aβ40 after 6 h, upon staining with ThT (Figure 4). Aβ40 mostly appeared as long fibril bundles (10−50 μm) organized as "sticks" similar to the amyloid fibers of other different proteins[33] (Figure 4a,b). In contrast, FA treatment led to the increase in amorphous, less-ordered Aβ40 aggregates (Figure 4c,d). These findings suggest a pivotal role of FA in perturbing the morphology of large Aβ40 assemblies. The high ThT fluorescence intensity signal measured in both cases indicates that no major differences exist for the ThT interaction with the hydrophobic binding sites of FA-Aβ40 aggregates and those of Aβ40 fibrils.

The peptide conformation evolution during the aggregation process was analyzed by FTIR (Figure 5). In agreement with our previous results,[28,29] FTIR quantitative analysis evidenced a prevalent random coil conformation of Aβ40 at t = 0 without FA. In the absence of FA, after 6 h, random coil was almost completely converted into β sheets and α helices. On the contrary, in the presence of FA, already at t = 0, and even more after 6 h, the secondary structure of Aβ40 was mainly composed of β sheets and turn percentage increased two-

dx.doi.org/10.1021/jp4079986 | J. Phys. Chem. B XXXX, XXX, XXX−XXX

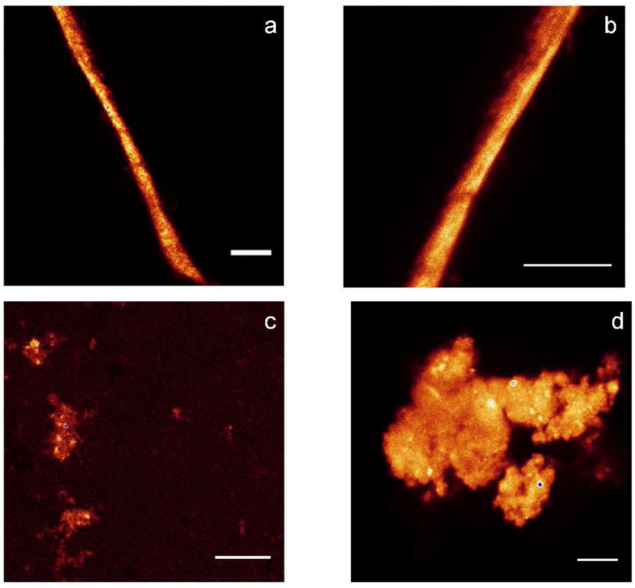

Figure 4. Fluorescence confocal images of ThT-stained Aβ40 (a,b) and FA-treated Aβ40 (c,d) at t = 6 h. Scale bar: 5 μm.

fold. After 6 h of incubation with FA, turn structures detected at t = 0 converted into β sheets and α helices. These results indicate that FA interacts with Aβ40 at its initial stage of aggregation promoting β-structure formation.

PICUP followed by SDS-PAGE and silver staining is a well-established technique for studying Aβ oligomerization.[34] Because oligomer assembly is a dynamic process where several molecular forms may exist simultaneously, this method provides quantitative snapshots of the different species present in the mixture at different times. As shown in Figure 6, in the absence of cross-linking, only Aβ40 monomers were observed (lane 2). After cross-linking, Aβ40 at t = 0 existed as a mixture of monomers and oligomers of orders 2−5 (lane 3). As the

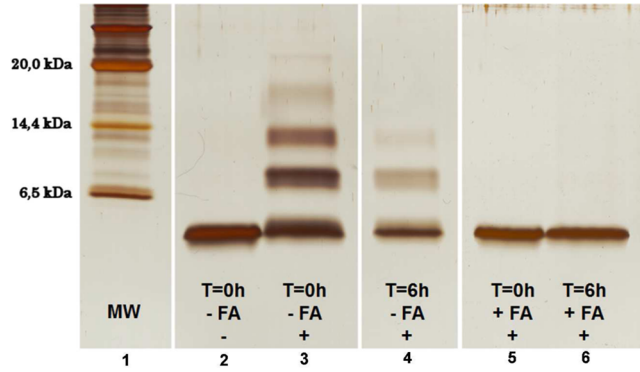

Figure 6. SDS-PAGE of Aβ40. Lane 2: t = 0, no cross-linking; lane 3: t = 0, cross-linked; lane 4: t = 6 h, cross-linked; lane 5: t = 0 + 330 μM FA, cross-linked; lane 6: t = 6 h + 330 μM FA, cross-linked.

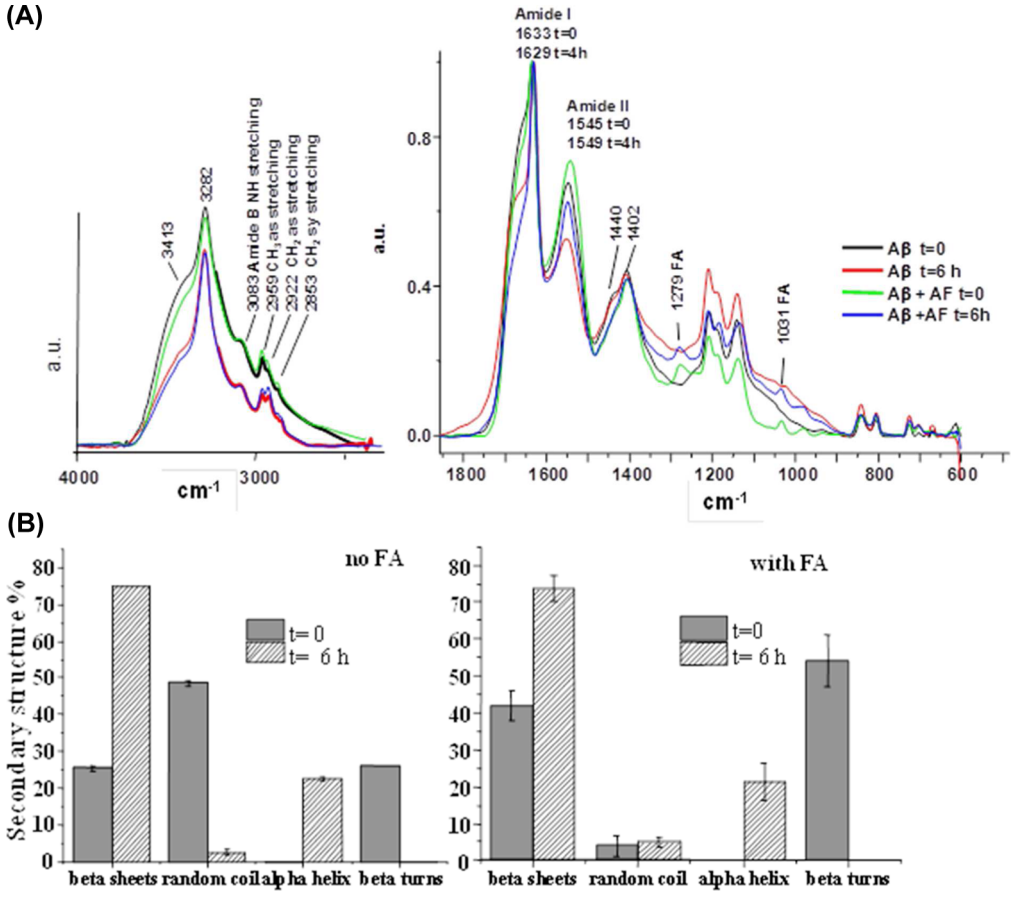

Figure 5. (A) FTIR absorption spectra in the 1850−600 and 4000−2500 cm^{-1} regions of Aβ40 and Aβ40+FA films obtained at t = 0 and 6 h. (B) Secondary structure percentages resulting from the deconvolution procedure applied to the amide I region of the FTIR spectra of Aβ40 with and without 330 μM FA at t = 0 and 6 h (N = 3 independent samples for each experimental condition).

dx.doi.org/10.1021/jp4079986 | J. Phys. Chem. B XXXX, XXX, XXX−XXX

incubation time proceeded, the monomer and oligomer concentration decreased in favor of mature fibrils (lane 4), which remained at the top of gel because of their sizes. The oligomer formation was perturbed and blocked by 330 μM FA (lane 5 and 6) and only monomers were detected. Conversely, large aggregates of FA-treated Aβ40 could not be detected. It should be noted that Ono et al. reported similar results although obtained under different experimental conditions.[25] This consistency supports the key interfering role of FA in the Aβ oligomerization process.

SEC analysis of the soluble part of the same samples showed that under our experimental conditions at t = 0 Aβ40 mainly eluted as single peak with an apparent MW corresponding to a trimer. The small peak around 4.62 min was due to soluble residual aggregates (Figure 7, curve a). The discrepancy

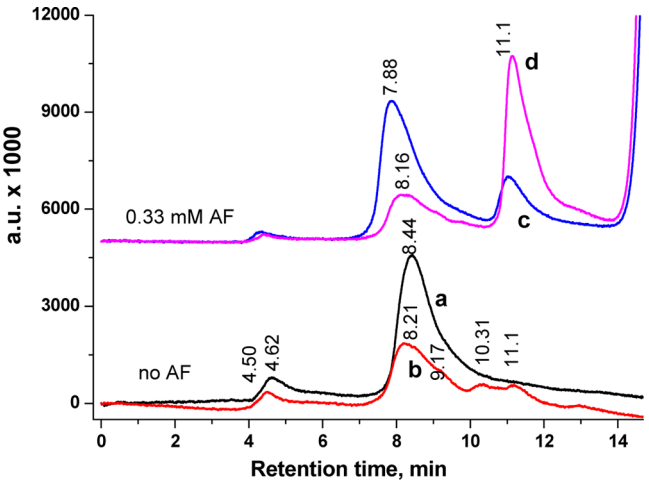

Figure 7. Absorbance SEC chromatograms at 280 nm of soluble fraction of 75 μM Aβ40 in 0.15 M NaCl at t = 0 without (a) and with 330 μM FA (c), after 6 h incubation at 45 °C without FA (b), and with 330 μM FA (d).

between this result and PICUP (Figure 6, lane 2) is ascribable to the nonideal chromatographic behavior of amphipathic peptides, such as Aβ40, which may establish both electrostatic and hydrophobic interactions with the column matrix generating different peaks ranging from 5 to 18 kDa (from monomer up to tetramer) in dependence of the solvents and columns used.[35] After 6 h of incubation, SEC chromatograms of Aβ40 without FA (Figure 7, curve b) showed a significant decrease in absorbance because of a lower fraction of soluble peptides. Small peaks corresponding to dimers (10.31 min) and monomers (11.1 min) appeared in agreement with PICUP results. In this case, at t = 6 h, the concentration of the Aβ40 soluble fraction is low enough to minimize the peptide interactions with the column matrix and thus to allow to detect monomers and dimers. In FA-treated Aβ40, two peaks corresponding to trimer and monomer species were detected, already at t = 0 (Figure 7, curve c). This result suggested that FA, interacting with Aβ40, could shield the peptide and avoid its interactions with column matrix, allowing its elution also as monomeric species. After 6 h of incubation (curve d in Figure 7), the monomer peak increased and the small peak of trimer at 7.88 min drastically decreased, indicating the reversal of Aβ40 oligomerization. However, on the basis of the time evolution of the peak area values we can state that the majority of the monomers did not result from the disassembling of oligomers but rather from the progressive, FA-induced solubilization of large aggregates. The amount of aggregates, under our experimental conditions, remains so high that no significant decrease in ThT fluorescence can be detected.

CONCLUSIONS

These experiments clearly showed that despite the formation of ThT fluorescent aggregates in both samples at the end of the kinetics the amyloid structures obtained with FA were different and more soluble than ordinary fibril bundles. This result represents an important warning because a positive ThT assay does not necessarily mean that fibrillar amyloid assemblies characteristic of AD are present. In fact, ThT is also capable of binding to nonfibrillar hydrophobic pockets in globular proteins[36−38] and β-sheet rich fibril precursors.[39] It is worth noting that almost simultaneously Cui et al.,[40] using the more fibrillogenic amyloid peptide Aβ42 and a different peptide preparation, showed that FA inhibits the formation of Aβ42 oligomers while accelerating the transition from Aβ42 oligomers to fibrils. Altogether, our and Cui et al.'s results provide a more comprehensive view of the effects of FA on amyloidogenesis related to AD and highlight the intrinsic variability of the assembly process. In particular, our study demonstrates that FA interacts with Aβ40 in the initial stage of the aggregation process and it interferes with the peptide self-assembly, redirecting it to the formation of nonfibrillar amorphous aggregates. At the molecular level, these complexes possess a β-structure conformation (as witnessed by ThT binding and FTIR), but they are more prone to be destabilized into monomeric species. These our findings represent a relevant step toward the comprehension of the molecular mechanisms of the antiamyloidogenic and neuroprotective activity of small phenolic molecules like FA and are meant to lead to novel more effective and selective drugs against amyloidogenesis.

AUTHOR INFORMATION

Corresponding Author

*E-mail: antonella.sgarbossa@nano.cnr.it; antonella.sgarbossa@pi.ibf.cnr.it. Tel: +390503153021. Fax: +390503152760.

Notes

The authors declare no competing financial interest.

ACKNOWLEDGMENTS

The present work was supported by a Grant from the Italian Ministry of University and Scientific Research for Programs of Relevant National Interest (PRIN 2008-prot.20083Y34Y7) "Development of a molecular strategy for the prevention of protein aggregation and fibrillogenesis: a biophysical approach".

REFERENCES

(1) Funato, H.; Yoshimura, M.; Kusui, K.; Tamaoka, A.; Ishikawa, K.; Ohkoshi, N.; Namekata, K.; Okeda, R.; Ihara, Y. Quantitation of Amyloid Beta-Protein (A Beta) in the Cortex During Aging and in Alzheimer's Disease. *Am. J. Pathol.* **1998**, *152*, 1633−1640.

(2) Huang, Y.; Mucke, L. Alzheimer Mechanisms and Therapeutic Strategies. *Cell* **2012**, *148*, 1204−1222.

(3) Chiti, F.; Dobson, C. M. Protein Misfolding, Functional Amyloid, and Human Disease. *Annu. Rev. Biochem.* **2006**, *75*, 333−366.

(4) Chimon, S.; Shaibat, M. A.; Jones, C. R.; Calero, D. C.; Aizezi, B.; Ishii, Y. Evidence of Fibril-Like Beta-Sheet Structures in a Neurotoxic

dx.doi.org/10.1021/jp4079986 | J. Phys. Chem. B XXXX, XXX, XXX−XXX

Amyloid Intermediate of Alzheimer's Beta-Amyloid. *Nat. Struct. Mol. Biol.* **2007**, *14*, 1157−1164.
(5) Cleary, J. P.; Walsh, D. M.; Hofmeister, J.; Shankar, M. G.; Kuskowski, M.; Selkoe, D. J.; Ashe, K. H. Natural Oligomers of the Amyloid-Beta Protein Specifically Disrupt Cognitive Function. *Nat. Neurosci.* **2005**, *8*, 79−84.
(6) Lashuel, H. A.; Lansbury, T., Jr. Are Amyloid Diseases Caused By Protein Aggregates That Mimic Bacterial Pore-Forming Toxins? *Q. Rev. Biophys.* **2006**, *39*, 167−201.
(7) Bucciantini, M.; Nosi, D.; Forzan, M.; Russo, E.; Calamai, M.; Pieri, L.; Formigli, L.; Quercioli, F.; Soria, S.; Pavone, F.; et al. Toxic Effects of Amyloid Fibrils on Cell Membranes: the Importance of Ganglioside GM1. *FASEB J.* **2012**, *26*, 818−831.
(8) Lee, C. C.; Nayak, A.; Sethuraman, A.; Belfort, G.; McRae, G. J. A Three-Stage Kinetic Model of Amyloid Fibrillation. *Biophys. J.* **2007**, *92*, 3448−345.
(9) Biancalana, M.; Koide, S. Molecular Mechanism of Thioflavin-T Binding to Amyloid Fibrils. *Biochim. Biophys. Acta* **2010**, *1804*, 1405−1412.
(10) Di Carlo, M.; Giacomazza, D.; San Biagio, P. L. Alzheimer's Disease: Biological Aspects, Therapeutic Perspectives and Diagnostic Tools. *J. Phys.: Condens. Matter* **2012**, *24*, 244102.
(11) Chopra, K.; Misra, S.; Kuhad, A. Current Perspectives on Pharmacotherapy of Alzheimer's Disease. *Expert Opin. Pharmacother.* **2011**, *12*, 335−350.
(12) Mecocci, P.; Polidori, M. C. Antioxidant Clinical Trials in Mild Cognitive Impairment and Alzheimer's Disease. *Biochim. Biophys. Acta* **2012**, *1822*, 631−638.
(13) Hawkes, C. A.; Ng, V.; McLaurin, J. A. Small Molecule Inhibitors of Aβ-Aggregation and Neurotoxicity. *Drug Dev. Res.* **2009**, *70*, 111−124.
(14) Joynera, P. M.; Cichewicz, R. H. Bringing Natural Products into the Fold − Exploring the Therapeutic Lead Potential of Secondary Metabolites for the Treatment of Protein-Misfolding Related Neurodegenerative Diseases. *Nat. Prod. Rep.* **2011**, *28*, 26−47.
(15) Sgarbossa, A. Natural Biomolecules And Protein Aggregation: Emerging Strategies Against Amyloidogenesis. *Int. J. Mol. Sci.* **2012**, *13*, 17121−17137.
(16) Mancuso, C.; Siciliano, R.; Barone, E.; Preziosi, P. Natural Substances and Alzheimer's Disease: From Preclinical Studies to Evidence Based Medicine. *Biochim. Biophys. Acta* **2012**, *1822*, 616−624.
(17) Ou, S.; Kwok, K.-C. Ferulic Acid: Pharmaceutical Functions, Preparation and Applications in Foods. *J. Sci. Food Agric.* **2004**, *84*, 1261−1269.
(18) Barone, E.; Calabrese, V.; Mancuso, C. Ferulic Acid and its Therapeutic Potential as a Hormetin for Age-Related Diseases. *Biogerontology* **2009**, *10*, 97−108.
(19) Fetoni, A. R.; Mancuso, C.; Eramo, S. L. M.; Ralli, M.; Piacentini, R.; Barone, E.; Paludetti, G.; Troiani, D. *In Vivo* Protective Effect of Ferulic Acid Against Noise-Induced Hearing Loss in the Guinea-Pig. *Neuroscience* **2010**, *169*, 1575−1588.
(20) Kim, H. S.; Cho, J. Y.; Kim, D. H.; Yan, J. J.; Lee, H. K.; Suh, H. W. Inhibitory Effects of Long Term Administration of Ferulic Acid on Microglial Activation Induced by Intercerebroventricular Injection of Beta Amyloid Peptide (1−42) in Mice. *Biol. Pharm. Bull.* **2004**, *27* (1), 120−121.
(21) Picone, P.; Bondi, M. L.; Montana, G.; Bruno, A.; Pitarresi, G.; Giammona, G.; Di Carlo, M. Ferulic Acid Inhibits Oxidative Stress and Cell Death Induced By Aβ Oligomers: Improved Delivery by Solid Lipid Nanoparticles. *Free Radical Res.* **2009**, *43* (11), 1133−1145.
(22) Ono, K.; Yoshiike, Y.; Takashima, A.; Hasegawa, K.; Naiki, H.; Yamada, M. Potent Antiamyloidogenic and Fibril-Destabilizing Effects of Polyphenols *in vitro*: Implications for the Prevention and Therapeutics of Alzheimer's Disease. *J. Neurochem.* **2003**, *87*, 172−181.
(23) Ono, K.; Hasegawa, K.; Yoshiike, Y.; Takashima, A.; Yamada, M.; Naiki, H. Nordihydroguaiaretic Acid Potently Breaks Down Pre-Formed Alzheimer's Beta-Amyloid Fibrils *in vitro*. *J. Neurochem.* **2002**, *81*, 434−440.
(24) Ono, K.; Hirohata, M.; Yamada, M. Ferulic Acid Destabilizes Preformed Beta-Amyloid Fibrils *in vitro*. *Biochem. Biophys. Res. Commun.* **2005**, *336*, 444−449.
(25) Ono, K.; Li, L.; Takamura, Y.; Yoshiike, Y.; Zhu, L.; Han, F.; Mao, X.; Ikeda, T.; Takasaki, J.; Nishijo, H.; et al. Phenolic Compounds Prevent Amyloid Beta-Protein Oligomerization and Synaptic Dysfunction by Site-specific Binding. *J. Biol. Chem.* **2012**, *287*, 14631−14643.
(26) Sgarbossa, A.; Monti, S.; Lenci, F.; Bramanti, E.; Bizzarri, R.; Barone, V. The Effects of Ferulic Acid on β-Amyloid Fibrillar Structures Investigated through Experimental and Computational Techniques. *Biochim. Biophys. Acta* **2013**, *1830*, 2924−2937.
(27) Fezoui, Y.; Hartley, D.; Harper, J.; Khurana, D.; Walsh, R.; Condron, M. M.; Selkoe, D.; Lansbury, P. T. J.; Fink, A.; Teplow, D. B. An Improved Method of Preparing the Amyloid β-Protein for Fibrillogenesis and Neurotoxicity Experiments. *Amyloid* **2000**, *7*, 166−178.
(28) Sgarbossa, A.; Buselli, D.; Lenci, F. *In vitro* Perturbation of Aggregation Processes in Beta-Amyloid Peptides: A Spectroscopic Study. *FEBS Lett.* **2008**, *582*, 3288−3292.
(29) Bramanti, E.; Lenci, F.; Sgarbossa, A. Effects of Hypericin on the Structure and Aggregation Properties of Beta-Amyloid Peptides. *Eur. Biophys. J.* **2010**, *39*, 1493−1501.
(30) Fancy, D. A.; Kodadek, T. Chemistry for the Analysis of Protein−Protein Interactions: Rapid and Efficient Cross-Linking Triggered by Long Wavelength Light. *Proc. Natl. Acad. Sci. U.S.A.* **1999**, *96*, 6020−6024.
(31) Bramanti, E.; Bramanti, M.; Stiavetti, P.; Benedetti, E. A Frequency Deconvolution Procedure Using a Conjugate-Gradient Minimization Method with Suitable Constraints. *J. Chemom.* **1994**, *8*, 409−421.
(32) Bramanti, E.; Ferrari, C.; Angeli, V.; Onor, M.; Synovec, R. E. Characterization of BSA Unfolding and Aggregation Using a Single-Capillary Viscometer and Dynamic Surface Tension Detector. *Talanta* **2011**, *85* (5), 2553−2561.
(33) Zhao, H.; Tuominen, E. K. J.; Kinnunen, P. K. J. Formation of Amyloid Fibers Triggered by Phosphatidylserine-Containing Membranes. *Biochemistry* **2004**, *43*, 10302−10307.
(34) Bitan, G.; Teplow, D. B. Rapid Photochemical Cross-Linking-A New Tool for Studies of Metastable, Amyloidogenic Protein Assemblies. *Acc. Chem. Res.* **2004**, *37*, 357−364.
(35) Walsh, D. M.; Lomakin, A.; Benedek, G. B.; Condron, M. M.; Teplow, D. B. Amyloid Beta-Protein Fibrillogenesis—Detection of a Protofibrillar Intermediate. *J. Biol. Chem.* **1997**, *272*, 22364−22372.
(36) Harel, M.; Sonoda, L. K.; Silman, I.; Sussman, J. L.; Rosenberry, T. L. Crystal Structure of Thioflavin T Bound to the Peripheral Site of *Torpedo californica* Acetylcholinesterase Reveals How Thioflavin T Acts as a Sensitive Fluorescent Reporter of Ligand Binding to the Acylation Site. *J. Am. Chem. Soc.* **2008**, *130*, 7856−7861.
(37) Groenning, M.; Olsen, L.; van de Weert, M.; Flink, J. M.; Frokjaer, S.; Jorgensen, F. S. Study on the Binding of Thioflavin T to Beta-Sheet-Rich and Non-Beta-Sheet Cavities. *J. Struct. Biol.* **2007**, *158*, 358−369.
(38) Sen, P.; Fatima, S.; Ahmad, B.; Khan, R. H. Interactions of Thioflavin T with Serum Albumins: Spectroscopic Analyses. *Spectrochim. Acta, Part A.* **2009**, *74*, 94−99.
(39) Chimon, S.; Shaibat, M. A.; Jones, C. R.; Calero, D. C.; Aizezi, B.; Ishii, Y. Evidence of Fibril-like β-sheet Structures in a Neurotoxic Amyloid Intermediate of Alzheimer's β-amyloid. *Nat. Struct. Mol. Biol.* **2007**, *14*, 1157−1164.
(40) Cui, L.; Zhang, Y.; Cao, H.; Wang, Y.; Teng, T.; Ma, G.; Li, Y.; Li, K.; Zhang, Y. Ferulic Acid Inhibits the Transition of Amyloid-β42 Monomers to Oligomers but Accelerates the Transition from Oligomers to Fibrils. *J. Alzheimer's Dis.* **2013**, *37*, 19−28.